Journal of Magnetic Resonance **138,** 12–18 (1999)
Article ID jmre.1999.1719, available online at http://www.idealibrary.com on IDEAL®

^{87}Rb Spin Diffusion in Ferroelectric RbH_2PO_4 Studied by Two Dimensional Exchange NMR

P. M. Cereghetti and R. Kind

Institute of Quantum Electronics, ETH-Hönggerberg, CH-8093 Zurich, Switzerland

Received August 5, 1998; revised January 20, 1999

We separate the contributions of spectral spin diffusion and chemical exchange in the 2D exchange NMR spectra of ^{87}Rb in the pseudo-spin glass $Rb_{1-x}(ND_4)_xD_2PO_4$ by studying the ^{87}Rb spin diffusion in the isostructural compound RbH_2PO_4 at 85K, where the system is frozen in the ferroelectric phase state. The fact that the spin–diffusion time (T_{SD}) of a particular point in the 2D spectrum depends essentially on its distance from the diagonal, allowed, even for the case of an unresolved 2D spectrum, to determine T_{SD} as a function of the frequency separation Δ over two orders of magnitude. In accordance with existing theories, $T_{SD}^{-1}(\Delta)$ was found to be of Gaussian shape. However, we found huge discrepancies between the calculated and the experimentally determined second moments. This failure of the theory is not understood at present.

I. INTRODUCTION

The investigation of spectral spin diffusion (*1–3*) in solids by means of two-dimensional (2D) exchange (*4*) nuclear magnetic resonance (NMR) is important because this mechanism often masks the effects of slow chemical exchange which is in fact the true aim of such a study. The two mechanisms cannot be distinguished in a 2D exchange NMR spectrum without additional information. To separate the two effects one has first to consider their specific properties.

Chemical exchange and spectral spin diffusion depend differently on external parameters: (i) Chemical exchange is independent on the coordinate system (i.e. in nonmagnetic systems it is independent on the orientation of the external magnetic field $\mathbf{B}_0$), but strongly temperature dependent because of thermal activation. The evolution of the 2D-exchange NMR spectrum is governed by a single particle autocorrelation time τ_c. (ii) Spectral spin diffusion is the transfer of longitudinal spin order through a spin system via mutual spin flips. It can take place between *equivalent* spins in an energy conserving way, but also between *inequivalent* spins with energy conservation provided, e.g., by lattice vibrations, which indirectly introduce a certain temperature dependence. The responsible interaction is the so called spin–flip term in the nuclear dipole–dipole Hamiltonian. This term contains an angular dependence of the form $(3\cos^2\theta - 1)$, where θ is the angle between the external magnetic field $\mathbf{B}_0$ and the vector $\mathbf{r}$ connecting the interacting spins. It follows that spectral spin diffusion depends on the crystal orientation. This orientational dependence is strongly enhanced when the difference of the NMR frequencies of the interacting inequivalent spins also depends on the crystal orientation. This is the case in the presence of quadrupolar splitting. In a manner similar to the case of chemical exchange, we can define a characteristic time T_{SD} which is the correlation time of the mutual spin flips. While we can expect a single T_{SD} in a translational invariant system, a probability distribution of T_{SD}'s has to be expected in an inhomogeneous system because of lattice defects, disorder, etc.

The separation of the two effects in the case when the spin–flip correlation time T_{SD} is comparable to the single particle autocorrelation time τ_c is very time consuming because the number of 2D spectra to be recorded is multiplied by the number of different external parameter settings. Instead of studying the contribution of spin diffusion in a system where also chemical exchange is present, it is advisable to look for a related system where one of the mechanisms is certainly dominant.

We demonstrate this for the case of the pseudo-spin-glass $Rb_{1-x}(ND_4)_xD_2PO_4$ (D-RADP-*x*) (*5–7*) and the isostructural ferroelectric RbH_2PO_4 (RDP).

In D-RADP-*x* for $0.35 < x < 0.7$, chemical exchange persists down to very low temperatures. RDP, on the other hand, exhibits an order–disorder phase transition from a paraelectric (PE) phase to a ferroelectric (FE) one with a transition temperature $T_c = 147$ K. The phase transition is characterized by the ordering of the protons on the O–H $\cdots$ O bonds connected with the breaking of the PE tetragonal symmetry from $I\bar{4}2d$ to the orthorhombic FE symmetry $Fdd2$. Since the proton motion is the unique chemical exchange process present in the system and since it freezes-out at the phase transition, only spectral spin diffusion is left at low temperatures. Thus $T_{SD} \ll \tau_c$ in the ferroelectric phase of RDP. This means that any off-diagonal intensity in a 2D exchange NMR spectrum can safely be assigned to spectral spin diffusion.

Because of the structural similarity of RDP and D-RADP-*x* one can characterize ^{87}Rb spin diffusion in the RDP system and adapt the results to D-RADP-*x*. In this way the distinction

1090-7807/99 $30.00

between chemical exchange and spin diffusion in 2D NMR spectra of glassy D-RADP-*x* should be possible.

In the next section we shall present the theory necessary to investigate spectral spin diffusion between ^{87}Rb spins in FE RDP. Section III is devoted to the experimental part of this work. Section IV treats specifically the cases of intra- and interline spin diffusion in FE RDP. In Section V the experimental data are discussed and interpreted based on the cross relaxation theory.

II. THEORY

The interest in spin diffusion began with the discovery of heteronuclear cross-relaxation in the laboratory frame. Modern techniques like coherence transfer under magic angle spinning (MAS) conditions have kept this interest alive. A milestone in the understanding is certainly the work of Suter and Ernst (*1*) where spectral spin diffusion is treated in great detail. Nevertheless, we will show that the prediction of ^{87}Rb spin diffusion times in a system like ferroelectric RDP fails by orders of magnitude. The reason for this might be the presence of quadrupolar splitting and inhomogeneous line broadening, as well as the random distribution of ^{85}Rb and ^{87}Rb isotopes. ^{87}Rb has a natural abundance of 27.835%. Since the aim of this analysis is to use the results of RDP for the case of D-RADP-*x* for discriminating the effects of spectral spin diffusion and slow motion, a less rigorous description is sufficient. Following Goldman (*8*), the rate of mutual spin flips is of the order

$$W \sim \frac{2\ \mathrm{Tr}(\mathbf{V}^2)}{\mathrm{Tr}(\mathbf{I}_z^2)} \left(\frac{\pi}{2M_2}\right)^{1/2} \exp\left(-\frac{\Delta^2}{2M_2}\right), \qquad [1]$$

where $\Delta = 2\pi\delta\nu_{jk}$ is the difference of the resonance frequencies ν_j and ν_k of the spins j and k ($\delta\nu_{jk} = |\nu_j - \nu_k|$), respectively, and the second moment M_2 is given by

$$M_2 = -\frac{\mathrm{Tr}([\mathcal{H}'_D, \mathbf{V}]^2)}{\mathrm{Tr}(\mathbf{V}^2)} \qquad [2]$$

with

$$\mathcal{H}'_D = \mathrm{K} \sum_{j\neq k} \frac{(1-3\ \cos^2\theta_{jk})}{r_{jk}^3}\, \mathbf{I}_z^j \mathbf{I}_z^k, \qquad [3]$$

$$\mathbf{V} = -\frac{K}{4} \sum_{j\neq k} \frac{(1-3\ \cos^2\theta_{jk})}{r_{jk}^3} (\mathbf{I}_+^j \mathbf{I}_-^k + \mathbf{I}_-^j \mathbf{I}_+^k), \qquad [4]$$

$$K = \frac{\mu_0}{4\pi}\gamma^2\hbar, \qquad [5]$$

where θ_{jk} is the angle between the external magnetic field $\mathbf{B}_0$ and the vector $\mathbf{r}_{jk}$ connecting the two nuclear spins j and k. γ is the gyromagnetic ratio of the ^{87}Rb spins involved.

The spin diffusion rate is here described as a product of a normalized Gaussian expressing the dependence on the angular frequency difference Δ and a factor containing the flip–flop term of the dipole–dipole interaction. The Gaussian can be thought of as resulting from an overlap integral of two Gaussians with variance $M_2/2$ and a frequency separation Δ.

Since we are interested only in the central line of the ^{87}Rb quadrupolar spectrum, we evaluated the traces in Eqs. [1] and [2] taking into consideration exclusively the mutual spin flips between the states $\pm\frac{1}{2}$. The rate of mutual spin flips W and the second moment M_2 are then expressed as

$$W \sim 5S_2(\vartheta,\ ^{87}\mathrm{Rb}) \left(\frac{\pi}{2M_2}\right)^{1/2} \exp\left(-\frac{\Delta^2}{2M_2}\right) \qquad [6]$$

with

$$M_2 = 1.2\, \frac{S_4(\vartheta,\ ^{87}\mathrm{Rb})}{S_2(\vartheta,\ ^{87}\mathrm{Rb})}. \qquad [7]$$

The numerical coefficient in Eq. [6] has its origin from

$$\frac{2\mathrm{Tr}(\mathbf{V}^2)}{\mathrm{Tr}(\mathbf{I}_z^2)} = 5S_2(\vartheta,\ ^{87}\mathrm{Rb}) \qquad [8]$$

in the case of mutual spin flips between the states $\pm\frac{1}{2}$, while S_2 and S_4 are lattice sums over the ^{87}Rb sites defined as

$$S_2(\vartheta) = K^2 \sum_{j\neq k} \frac{(1-3\ \cos^2\theta_{jk})^2}{r_{jk}^6} \qquad [9]$$

$$S_4(\vartheta) = K^4 \sum_{j\neq k} \frac{(1-3\ \cos^2\theta_{jk})^4}{r_{jk}^{12}}, \qquad [10]$$

where ϑ is the angle between $\mathbf{B}_0$ and the c-axis of the crystal.

For the numerical calculation of S_2 and S_4 we have chosen the origin of the coordinate system to coincide with the spin k. Around this site the Rb lattice was constructed. In order to have convergence of the sums S_2 and S_4 it was sufficient to sum over $5 \times 5 \times 5 = 125$ unit cells. Because of the ^{87}Rb natural abundance, only a fraction of 27.835% of ^{87}Rb nuclear spins contributes to S_2 and S_4. Taking all this into consideration, we have performed Monte Carlo simulations generating random distributions of ^{87}Rb on Rb sites with a probability of 0.27835. For each configuration, we have calculated M_2, $2\mathrm{Tr}(\mathbf{V}^2)/\mathrm{Tr}(\mathbf{I}_z^2)$, and $W(\Delta = 0)$ from Eqs. [6–8], using Eqs. [9] and [10]. The final results were obtained from averaging over 10000 random configurations. They are depicted in Fig. 5 and will be discussed in Section V.

III. EXPERIMENTAL

The single crystals of RDP were grown from an aqueous solution using a standard convection technique (*9*). The spin diffusion measurements were made with a home-built NMR-spectrometer in a $\mathbf{B}_0$-field of 7 *T* on ^{87}Rb nuclear spins ($I = \frac{3}{2}$). The temperature was stabilized at 85 K in a continuous-flow cryostat with an accuracy of about ± 0.05 K. We used a standard exchange pulse sequence with echo detection (4) 90_x–t_1–90_{-x}–τ_m–90_x–d–90_x–*echo* measured with appropriate phase cycling to remove unwanted signals caused by pulse imperfections and higher order echoes. For mixing times less than 1 ms it was not possible to completely avoid phase distortions because of nonrelaxed coherences which cannot be removed by phase cycling. For long mixing times, $\tau_m > 7$ s, the longitudinal spin lattice relaxation reduced drastically the signal to noise ratio. The mixing time τ_m was incremented from 1 ms to 7 s.

We evaluate the spectral spin diffusion of ^{87}Rb ($I = \frac{3}{2}$) using 2D-exchange NMR spectroscopy on the $+\frac{1}{2} \leftrightarrow -\frac{1}{2}$ transitions in FE RDP. This central transition is subjected to second order nuclear quadrupole shifts, which depend on the relative orientation between the external field $\mathbf{B}_0$ and the electrical field gradient (EFG) tensor at the site of the nucleus. For symmetry reasons a line splitting occurs at the PE–FE phase transition. Furthermore, an inhomogeneous broadening of the line is observed (*5*).

During the measurements the crystallographic a-axis was perpendicular to the external magnetic field $\mathbf{B}_0$ and the c-axis was tilted 7° away from it. At this orientation the 1D spectrum of FE RDP exhibits two distinct resonance lines (Fig. 1a), with a frequency separation that can be calculated from the crystal orientation (*5*). For this particular orientation it amounts to $\Delta\nu_{res} = 6.2$ kHz.

The FE RDP structure consists of stacked Rb–PO_4 layers which are related by "diamond" glide planes (e.g. $\{m_{xy}|0, \frac{1}{2}, \frac{1}{4}\}$). Applying this symmetry element twice yields the translation $\{1|\frac{1}{2}, \frac{1}{2}, \frac{1}{2}\}$ which is one of the basis vectors of the primitive unit cell. From this follows that there are four formula units ($Z = 4$) in the conventional body centered unit cell.

Since the EFG tensor is invariant under basic translations we find the same EFG tensor alternatively in every second layer of the Rb sublattice (Fig. 1b). As a consequence two Rb-NMR lines are observed in the FE phase, which can be assigned to the two different layer types. Due to crystal imperfections the two lines are inhomogeneously broadened. Spectral spin diffusion can thus take place either among equivalent ^{87}Rb spins or among inequivalent ones, so that we can distinguish between intraline and interline spin diffusion, respectively. Earlier measurements in our group (*6, 7*) revealed a strong orientational dependence of the interline spin diffusion time. This can be explained by the change of the interline frequency splitting Δ on increasing the tilt angle ϑ. The corresponding data are shown in the overview Fig. 5. However, they were not

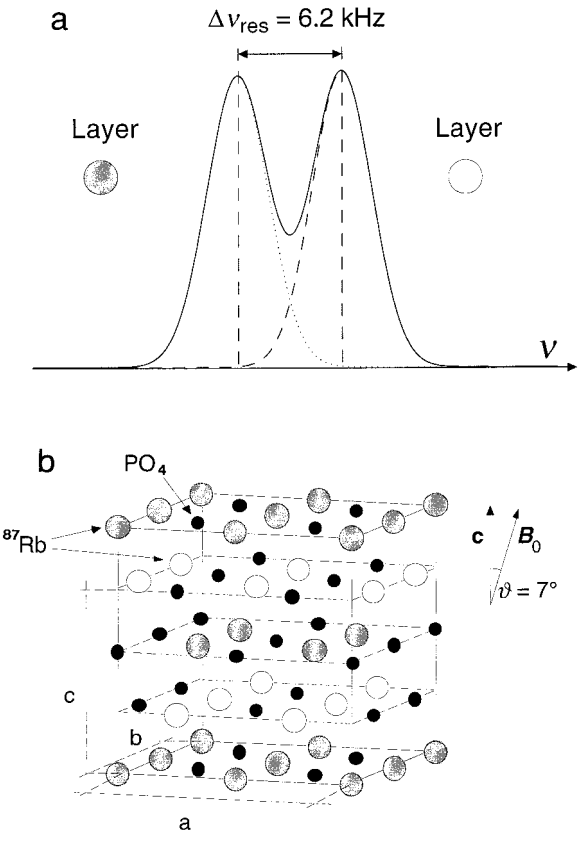

FIG. 1. (a) Quadrupolar splitted central line of the ^{87}Rb 1D NMR spectrum. (b) Rubidium sublattice (white and black large balls) and PO_4 groups (black small balls) in FE RDP. The inset shows the orientation of $\mathbf{B}_0$ with respect to the *c*-axis.

suitable for the main purpose of this work, namely to estimate the spin diffusion time for $\Delta = 0$.

Figure 2 shows the evolution of the 2D spectrum in the form of contour-plots for three different mixing times. For increasing mixing times the diagonal peaks change from an ellipsoidal shape ($\tau_m = 1$ ms) to a circular one ($\tau_m = 500$ ms). This is due to spin diffusion among equivalent spins resulting in the growth of intraline cross peaks. Circular cross sections are obtained only for Gaussian 1D line shapes.

Figure 3a shows a 2D exchange spectrum taken for a mixing time of 500 ms with the projection of the cross section of a diagonal peak perpendicular to the diagonal. This cross section consists of a distribution of homogeneous lines with the widths at half height (HWHM) corresponding to the inverse transverse relaxation time T_2^{-1}. Except for the very central line, all other lines are intraline cross peaks caused by spin diffusion.

The onset of interline spin diffusion becomes visible for $\tau_m > 200$ ms in the form of resolved cross peaks as shown in Fig. 2 for $\tau_m = 5$ s. Figure 3b displays a cross section through the top of the two inhomogeneously broadened cross peaks. These inhomogeneous cross peaks are a superposition of homogeneous cross peaks resulting from mutual spin flips of physically

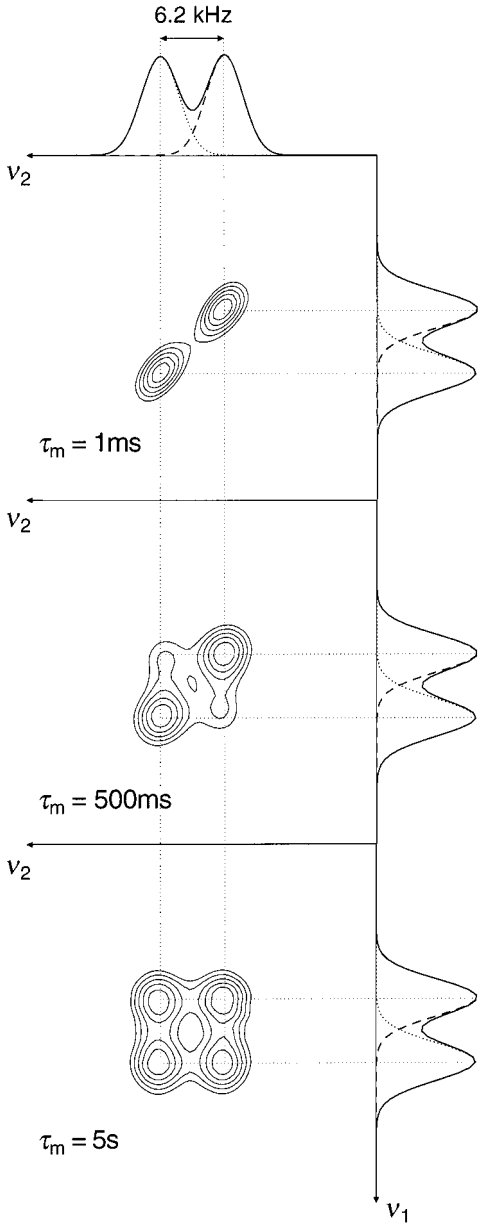

FIG. 2. Contour plots of 2D NMR exchange spectra for three different mixing times. The diagonal peaks change from an ellipsoidal shape (τ_m = 1 ms) to a circular one (τ_m = 500 ms) because of spin diffusion among equivalent spins. The onset of interline spin diffusion becomes visible for τ_m > 200 ms in the form of distinct inhomogeneously broadened cross-peaks.

inequivalent ^{87}Rb spin pairs. They appear at coordinates (ν_1, ν_2) and (ν_2, ν_1) in the 2D plot, where ν_1 and ν_2 are the individual resonance frequencies of the two spins.

IV. EVALUATION OF THE SPIN DIFFUSION TIMES

As already mentioned above and shown in Fig. 3a, the orthogonal broadening of the two diagonal peaks corresponds to the growth of intraline cross peaks. This growth begins close to the diagonal and moves further away from it with increasing τ_m. From this we conclude that we do not deal with a single spin diffusion time but with a distribution: the farther away from the diagonal, the higher T_{SD}. Similar to the inhomogeneously broadened 1D spectrum that is a superposition of narrow 1D Gaussians, the 2D exchange spectrum is a superposition of 2D Gaussians. We assume now that this continuous distribution of Gaussians can be replaced by a discrete distribution of equidistant Gaussians both in one and two dimensions. A similar discretisation is already obtained from the 2D Fourier transform. Moreover we assume that all of these 2D Gaussians are isolated from all neighbors as if they would not be there. These assumptions allow to treat the intraline spin diffusion like a set of interline spin diffusions. Possible drawbacks of this procedure will be discussed later.

Any pair of 2D Gaussians on the diagonal has a corresponding pair of off-diagonal 2D Gaussians, such that the four form a square in the ν_1, ν_2 plane. If we place the origin at the center of this square, the diagonal lines have the coordinates $(+\nu, +\nu)$ and $(-\nu, -\nu)$, the off-diagonal ones $(+\nu, -\nu)$ and $(-\nu, +\nu)$. The 1D-frequency separation of the two lines is thus 2ν, which yields, from Eq. [1], $\Delta = 4\pi\nu$. For symmetry reasons it is convenient to select an origin which coincides with one of the maxima of the diagonal spectrum. Then we have $I(+\nu, +\nu) = I(-\nu, -\nu)$ as long as the overlapping intensity of the second diagonal peak can be neglected. This choice of origin also defines the cross section through the peak as shown in Fig. 3a. The intensity ratio between the interacting diagonal 2D-Gaussians and the resulting off-diagonal 2D-Gaussians is given by (10)

$$R = \frac{I(\tau_m, +\nu, -\nu)}{I(\tau_m, +\nu, +\nu)} = \tanh \frac{\tau_m}{T_{SD}(\nu)}. \qquad [11]$$

For our purpose is more convenient to use an equivalent form of Eq. [11]

$$I(\tau_m, +\nu, -\nu) = \tfrac{1}{2} I_{tot}(\tau_m = 0, +\nu, +\nu) \times [1 - \exp(-2\tau_m/T_{SD}(\nu))], \qquad [12]$$

where I_{tot} is the total intensity involved in the exchange process.

Because of the origin choice the intensities of the interacting diagonal Gaussians are equal

$$I(\tau_m = 0, +\nu, +\nu) = I_{1D}(\nu) = I_{1D}(\nu = 0)\exp(-\nu^2/2\sigma_D^2) \qquad [13]$$

where the Gaussian can be fitted to the 1D inhomogeneously broadened NMR line we are considering, yielding a line width of $\sigma_D = 1.84 \pm 0.02$ kHz. It should be noted that not the whole intensity $I(\tau_m, +\nu, -\nu)$ is resulting from spin diffusion. In fact,

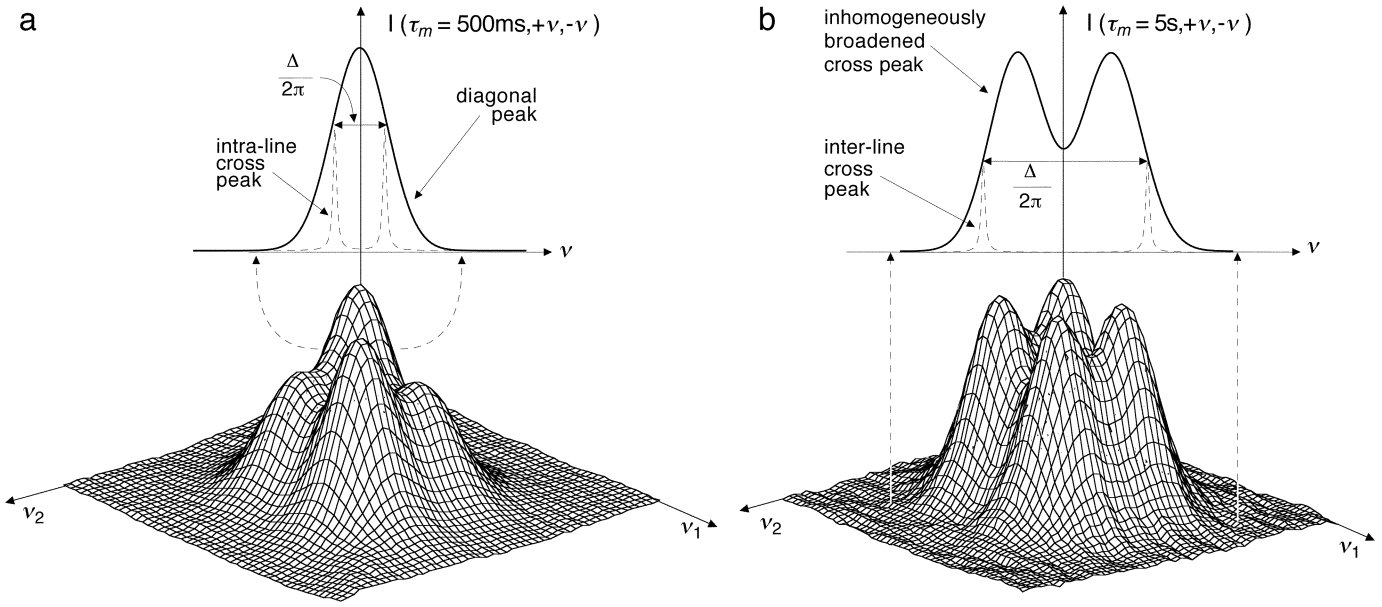

FIG. 3. (a) Intraline spectral spin diffusion cross peaks resulting from exchange between single homogeneously broadened lines for a mixing time $\tau_m = 500$ ms. Definition of $I^{intra}(\tau_m, +\nu, -\nu)$ as an orthogonal cut through a diagonal peak maximum. (b) Interline spectral spin diffusion cross peaks resulting from exchange between single homogeneously broadened lines for a mixing time $\tau_m = 5$ s. Definition of $I^{inter}(\tau_m, +\nu, -\nu)$ as an orthogonal cut through the global cross peaks maxima.

as illustrated in the leftmost contour plot of Fig. 2, even for the shortest mixing times there is a contribution to $I(\tau_m, +\nu, -\nu)$ because of dipolar broadening. $I(\tau_m \to 0, +\nu, -\nu)$ can be fitted very well by a Gaussian with a standard deviation $\sigma_0 = 0.68 \pm 0.02$ kHz. Since we can hardly predict how this intensity is reduced with growing τ_m, all fits with Eq. [12] were done for $|\nu| \geq 2$ kHz. The results are shown in Fig. 4, where the intraline spin diffusion time $T^{intra}_{SD,exp}$ (closed circles) is plotted vs ν. The negative or positive values of ν correspond to the left or right side of the diagonal, respectively. For $|\nu| > 5$ kHz the intensities are so weak that the results are not reliable anymore. Nevertheless $T^{intra}_{SD,exp}(\nu)$ can be fitted with an inverted Gaussian (Fig. 4, dashed curve):

$$T_{SD}(\nu) = T_{SD}(0)\exp(4\nu^2/2\sigma^2_{SD}) \qquad [14]$$

yielding $\sigma^{intra}_{SD,exp}$, of 3.93 ± 0.12 kHz and $T^{intra}_{SD,exp}(0) = 400 \pm 50$ ms.

For the interline spin diffusion the procedure is similar but the origin is now shifted to the middle of the two diagonal peaks (Fig. 3(b)). Since the intensity $I(\tau_m = 0, +\nu, -\nu)$ of the diagonal contribution is here much smaller, the fits with Eq. [12] give reasonably small error bars already for $|\nu| \geq 0.8$ kHz as shown in Fig. 4, where the interline spin diffusion time $T^{inter}_{SD,exp}$ we measured is indicated by open circles. Again, Eq. [14] (solid curve) is fitted to the data points, yielding $\sigma^{inter}_{SD,exp}$, of 5.78 ± 0.16 kHz and $T^{inter}_{SD,exp}(0) = 832 \pm 28$ ms.

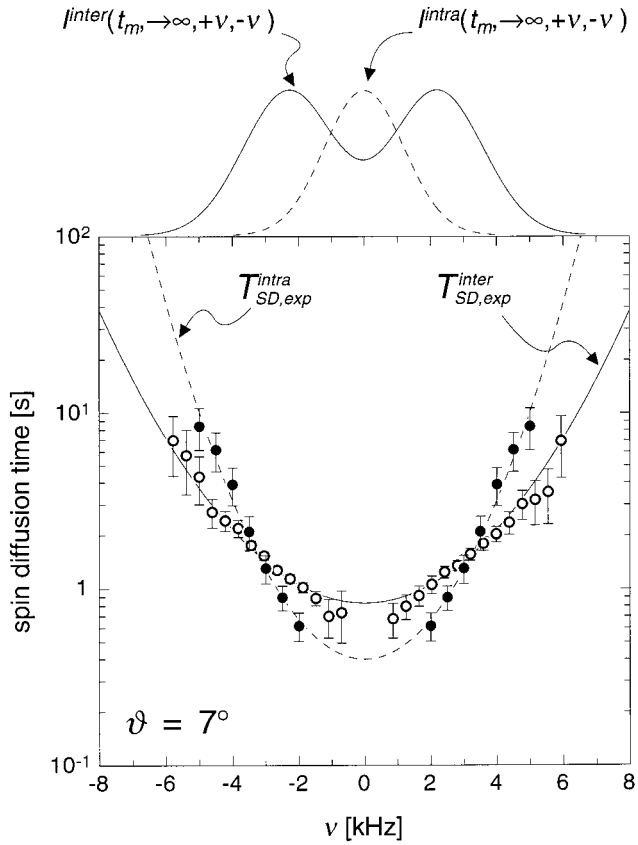

FIG. 4. ^{87}Rb spin diffusion times vs frequency in FE RDP. Closed circles: measured intraline spin diffusion times. Open circles: measured interline spin diffusion times. Curves are fits with Eq. [14].

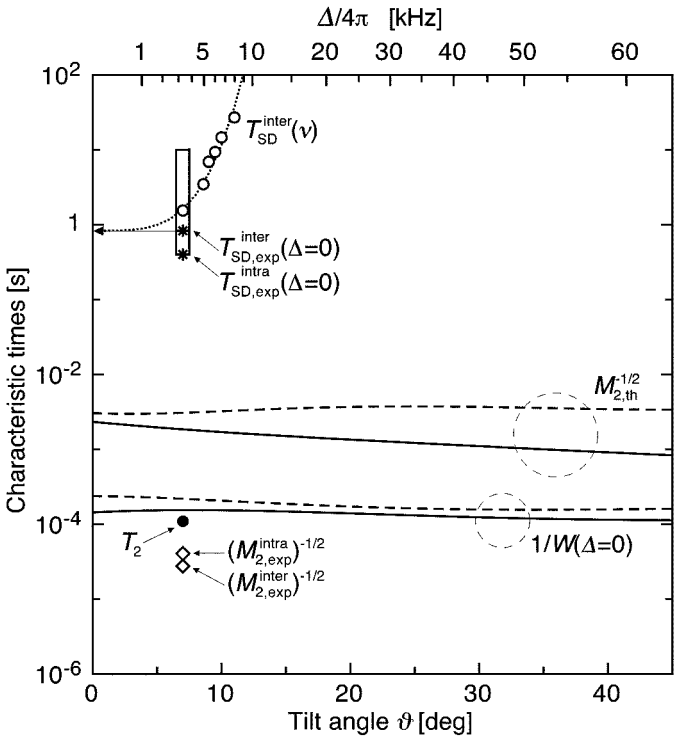

FIG. 5. Comparison of measured spin diffusion times in RDP (open circles, stars, rectangular band) with calculated values of $1/W$ for $\Delta = 0$ as a function of the tilt angle ϑ between the crystal c-axis and the external magnetic field $\mathbf{B}_0$ (dashed line: intraline spin diffusion; solid line: interline spin diffusion). The upper horizontal scale is the value of $\nu = \Delta/4\pi$ corresponding to the quadrupolar inter line splitting $\Delta(\vartheta)$. The dotted curve is the transformed right half of the solid curve of Fig. 4. The homogeneous T_2 (full circle) is compared with the experimental $M_2^{-1/2}$ (diamonds) and the calculated $(M_2(\vartheta))^{-1/2}$.

V. DISCUSSION

With the results of the previous section the main task of this investigation is fulfilled. We have obtained reliable values of $T_{SD,exp}$ for ^{87}Rb as a function of the line splitting 2ν, which can be adapted to the case of the proton glass D-RADP-50. However, it is interesting to know how far this behavior can be predicted from the theory of mutual spin flip presented in the theoretical section.

Figure 5 gives an overview of the experimental and theoretical results presented in Sections II to IV.

The fact that the experimental $T_{SD}(\nu)$ can be fitted very well with an inverted Gaussian proves that we deal with the overlap integral of two Gaussians as predicted by the theory. The corresponding dynamic second moments $M_2 = (2\pi\sigma)^2$ of Eqs. [1] and [6] are obtained from the fit of the measured spin diffusion times with Eq. [14]

$$M_{2,exp}^{intra} = (6.1 \pm 0.4) \times 10^8 \text{ rad}^2\,\text{s}^{-2}$$

$$M_{2,exp}^{inter} = (13.2 \pm 0.7) \times 10^8 \text{ rad}^2\,\text{s}^{-2}$$

These values are by three orders of magnitude higher than the ones calculated from Eq. [2] via Eq. [7]. In Figure 5 the inverse square roots of the experimental dynamic second moments $M_{2,exp}^{intra}$ and $M_{2,exp}^{inter}$ for a crystal orientation of $\vartheta = 7°$ are compared with the inverse square roots of the second moment results $M_{2,th}^{intra}$ and $M_{2,th}^{inter}$ from the Monte Carlo simulation. It is clear that these values are far from being of the same order of magnitude.

In Fig. 5 we give an overview over all relevant quantities for the spin diffusion process in RDP. The direct comparison is achieved by expressing all quantities in units of time. While the lines (solid, dashed, dotted) represent theoretical calculations, the data points are derived from measurements. The rectangular band contains the spin diffusion times derived in this work at the tilt angle $\vartheta = 7°$ according to Fig. 4. The two stars correspond to the extrapolation of the present measurements for $\Delta = 0$. The dotted line corresponds to the right half of the solid line in Fig. 4 using the transformed frequency scale (upper scala). The open circles represent earlier measurements performed in our group (6) of the interline spin diffusion time as a function of the tilt angle ϑ, which is the control parameter for the interline splitting Δ. The maximum measurable values of T_{SD} and with it the maximum tilt angle ($\vartheta = 11°$) was limited by T_1. These earlier measurements did not allow for an extrapolation to $\Delta = 0$. The two diamonds correspond to the fitted parameters $M_{2,exp}^{intra}$ and $M_{2,exp}^{inter}$ of Eq. 14, whereas the full circle is the measured homogeneous T_2. The evaluation of Eqs. [6] and [7] with the help of Monte Carlo lattice sums yielded the values of W and M_2 as a function of the tilt angle ϑ. The corresponding values for $\Delta = 0$ are shown for the cases of intraline (dashed lines) and interline (solid lines) interaction. They differ by orders of magnitude from the experimental values.

At present we do not have any explanation for this failure of the theory so that we are left with the following questions. Why is the apparent width of the two overlapping Gaussians obtained from the experimental dynamic second moments ($\sigma^{intra} = 2.8$ kHz, $\sigma^{inter} = 4$ kHz) even larger than the static inhomogeneous line width ($\sigma_D = 1.84$ kHz)? This fact violates our isolation assumption of the previous section. But exactly this assumption made the problem tractable at all. Another question concerns the influence of the temperature. How strong is the phonon assistance in spectral spin diffusion? Furthermore, we have to ask whether it is really harmless to neglect the satellite transitions in our treatment. We hope that our results and these open questions will stimulate further work in this field.

VI. CONCLUSION

Our calculation of the ^{87}Rb spin diffusion times T_{SD} in FE RDP proved that the function $T_{SD}^{-1}(\Delta)$ is a Gaussian (as predicted by the theory), where Δ is the angular frequency separation between the interacting spins. The particular situation in

FE RDP allowed that both intraline and interline spin diffusion times could be measured. However, discrepancies of more than three orders of magnitude were found between the theoretical and experimental values of the dynamic second moment M_2. In particular, we observed that the dynamic second moment exceeds the static inhomogeneous line width by a factor of 2.

ACKNOWLEDGMENTS

We thank Professor J. Dolinšek for the critical reading of the manuscript. This work was supported in part by the Swiss National Science Foundation.

REFERENCES

1. D. Suter and R. R. Ernst, *Phys. Rev. B* **25,** 6038–6041 (1982).
2. D. Suter and R. R. Ernst, *Phys. Rev. B* **32,** 5608–5627 (1985).
3. A. Abragam, "The Principles of Magnetic Resonance," Clarendon Press, Oxford (1961).
4. R. R. Ernst, G. Bodenhausen, and A. Wokaun, "Principles of Nuclear Magnetic Resonance in One and Two Dimensions," Clarendon Press, Oxford (1987).
5. N. Korner and R. Kind, *Phys. Rev. B* **49,** 5918 (1994).
6. N. Korner and R. Kind, *in* "Proceedings of the 26th Congress AMPERE on Magnetic Resonance" (A. Anagnostopoulos, F. Milia, and A. Simopoulos, Eds.), p. 601a, Athens (1992).
7. N. Korner, "From Long Range Order to Glass Order: Static and Dynamic Properties of the Solid Solution $Rb_{1-x}(ND_4)_xD_2PO_4$," Diss ETH No. 9952, Ph.D. dissertation, ETH, Zürich, (1993).
8. M. Goldman, "Spin Temperature and Nuclear Magnetic Resonance in Solids," Oxford University Press, Oxford, (1970).
9. H. Arend, R. Perret, H. Würst, and P. Kerkoč, *J. Cryst. Growth* **74,** 321 (1986).
10. J. Dolinšek, B. Zalar, and R. Blinc, *Phys. Rev. B* **50,** 805–821 (1994).